Role of Nanoparticles in Life Cycle of ZnO/Polyurethane Nanocomposites

Xiaohong Gu, Guodong Chen, Minhua Zhao, Stephanie. S. Watson, Paul E. Stutzman, Tinh Nguyen, Joannie W. Chin and Jonathan W. Martin

Materials and Construction Research Division
National Institute of Standards and Technology, Gaithersburg, MD 20899, USA
xiaohong.gu@nist.gov

ABSTRACT

This study investigated the role of ZnO nanoparticles in the photodegradation of a waterborne polyurethane (PU) nanocomposite during exposure to ultraviolet (UV) radiation. The effects of loading and size of ZnO nanoparticles on the photodegradation of ZnO/PU films were evaluated. Chemical and surface morphological changes of exposed specimens were examined by Fourier transform infrared spectroscopy (FTIR) and atomic force microscopy (AFM), respectively. The results clearly showed that ZnO nanoparticles can act as a photo-catalyst or a photo-stabilizer, depending on the UV exposure conditions. Both size and loading of the ZnO nanoparticles had a strong effect on photodegradation of the nanocomposites.The polymer in the vicinity of the nanoparticles preferentially degrades when the nanoparticles act as a photo-catalyst, and is shielded when they behave as a photo-stabilizer.

Keywords: nanoparticles, nanocomposites, UV exposure, life cycle, AFM

1 INTRODUCTION

Recent developments in nanoparticle technology have initiated the use of inorganic UV absorbers such as zinc oxide (ZnO) for UV protection of polymers [1]. This approach is based on the unique UV absorbing ability of these metal oxides. Compared to the traditional organic UV absorbers, the inorganic UV absorbers offer transparency in the visible range and are non-migratory in the polymer matrix. They also offer enhancements in electrical, mechanical, and antibacterial properties for the polymers [1]. However, due to the photoreactivity of some metal oxide nanoparticles [2], their contributions to UV protection of the polymeric matrix can be complicated.

In this paper, we have investigated the role of ZnO nanoparticles in the life-cycle of a waterborne PU nanocomposite exposed to UV radiation. Nano-filled polyurethane thin films were prepared with ZnO nanoparticles having various sizes and loadings. The UV exposure of the nanocomposites was conducted on both NIST SPHERE (**S**imulated **P**hotodegradation via **H**igh **E**nergy **R**adiant **E**xposure) and an UV/Ozone (UVO) chamber. Chemical changes of the nanocomposite films were examined by FTIR. Changes in film morphology were characterized by AFM. The photoreactivity of ZnO nanoparticles was measured by electron paramagnetic resonance *(EPR)* spectroscopy. The results clearly showed that the ZnO nanoparticles played a critical role in the life cycle of the ZnO/PU nanocomposites. They acted either as a photo-catalyst or a photo-stabilizer, depending on the UV exposure conditions. The degradation behavior of the polymers in the vicinity of the nanoparticles exposed to different conditions was discussed.

2 EXPERIEMNTALS*

2.1 Materials and Specimen Preparation

A commercial waterborne dispersion of polyurethane (PU, Bayer Material Science) and a series of waterborne dispersions of ZnO nanoparticles (BYK Additives & Instruments) were selected for preparing ZnO/PU nanocomposites. The PU dispersion was a one-component, anionic dispersion of an aliphatic polyester urethane resin in water/n-methyl-2-pyrrolidone solvent. The nominal average diameters of the ZnO nanoparticles were 20 nm, 40 nm, and 60 nm, and their respective specific surface areas were 54 m^2/g, 33 m^2/g and 18 m^2/g (as provided by the manufacturer).

ZnO/PU nanocomposite films (hereafter referred to as ZnO/PU films) were prepared by mixing the PU dispersion with different loadings and/or different sizes of ZnO nanoparticles using a mechanical stirrer (Dispermat, VMA) at 315 rad/s (3000 rpm) for 20 minutes. Three ZnO nanoparticle loadings, 1 %, 2 %, and 5 % (based on mass of the solid PU), were used for 20 nm ZnO nanoparticles. Similarly, three sizes of nanopartilces, 20 nm, 40 nm and 60 nm were used at 5 % loading. After degassing for 1 h in vacuum, the mixture was then applied to the substrates. Thin films having a thickness of approximately 5 μm were prepared by spin coating onto calcium fluoride (CaF_2) substrates. Thick films having a nominal thickness of approximately 100 μm were prepared by drawdown technique on a glass substrate that was pretreated with a release agent. All films were dried overnight under ambient conditions, followed by an oven post-curing at 150 °C for 10 min. Free-standing ZnO/PU films were obtained by removing the thick films from glass substrates. In addition,

PU films without ZnO nanoparticles were also prepared for comparison.

2.2 High UV Radiant Laboratory Exposure

UV exposure of ZnO/PU films was mainly conducted on the NIST SPHERE, a 2 m diameter integrating sphere-based weathering chamber. This weathering device utilizes a mercury arc lamp system that produces a collimated and highly uniform UV flux of approximately 480 W/m^2 in the spectral range between 295 nm and 400 nm. ZnO/PU films coated on CaF_2 were placed in two 17-window sample holders, and exposed to UV radiation at 45 °C, 0 % RH and 45 °C, 75 % RH. To study UV exposure conditions on the photo-catalytic effect of nanoparticles, ZnO/PU films were also exposed in an UV/Ozone (UVO) cleaner (Jetlight Company, Inc.). The main wavelengths of the light emission of this device are 254 nm and 185 nm.

2.3 Measurements

2.3.1 Fourier Transform Infrared Spectroscopy (FTIR)

Chemical degradation of the ZnO/PU films coated on CaF_2 was measured by transmission FTIR spectroscopy using a PIKE auto-sampling accessory (PIKE Technologies). This automated sampling device allows efficient and precise recording of transmission FTIR spectra. The auto-sampler accessory was placed in an FTIR spectrometer compartment (Thermo-Nicolet Nexus 670xl) equipped with a liquid nitrogen-cooled mercury cadmium telluride (MCT) detector. Spectra were recorded at a resolution of 4 cm^{-1} and were averaged over 128 scans. The peak height was used to represent IR intensity, which was expressed in absorbance units.

2.3.2 Atomic Force Microscopy (AFM)

A Dimension 3100 AFM (Veeco Metrology) was used to image the morphology and the microstructure of the ZnO/PU films before and after UV exposure. The AFM was operated in tapping mode using commercial silicon probes (Olympus AC-160TS) with a resonance frequency of approximately 300 kHz.

2.3.3 Dynamic Mechanical Thermal Analysis (DMTA)

The glass transition temperatures (T_g) of the ZnO/PU films were measured on an RSA III (TA Instruments) dynamic mechanical thermal analyzer (DMTA). Measurements were performed from - 100 °C to 150 °C at a temperature ramp of 3 °C/min, with a frequency of 1.0 Hz and a strain of 0.5 %. T_g was determined from the maximum of the tan δ peak, and was the average of three measurements.

2.3.4 Electron Paramagnetic Resonance (EPR) Spectroscopy

EPR analysis was conducted to quantify the photoreactivity of ZnO nanoparticles using radical spin traps 3-aminoproxyl (AP) (Aldrich) at 500 µmol/L in deionized water and stock preparations (0.2 g/L) of metal oxide suspensions in deionized water. For each spin trap experiment, a new mixture of spin trap stock solution and ZnO suspension was prepared to monitor the photo-initiated radicals under UV irradiation at ambient temperature. Aliquots (50 µL) of the spin trap/ZnO mixture were placed into EPR capillary tubes in the EPR cavity and irradiated *in situ* with a Xe arc lamp at 500 W. All EPR spectra were recorded at ambient conditions with a Bruker Elexsys E500 EPR spectrometer. Control experiments were carried out to ensure that observed EPR signals did not arise from photolysis or oxidation products of the spin traps themselves as well as to monitor the EPR signal stability in the dark and under illumination.

3. RESULTS AND DISCUSSION

3.1 Effect of Nanoparticles on Chemical and Thermo-mechanical Properties of ZnO/PU Films before UV Exposure

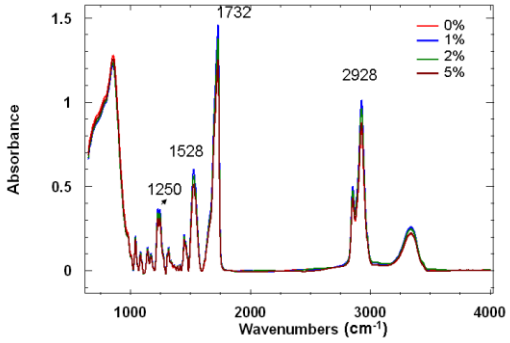

Figure 1: FTIR transmission spectra of pure PU and ZnO/PU films containing 1 %, 2 %, and 5 % ZnO loadings by mass. The specimens are spin-coated films on CaF_2 substrates.

Figure 1 displays the FTIR transmission spectra of unexposed ZnO/PU films having ZnO loadings of 0 %, 1 %, 2 %, and 5 % by mass. The ZnO/PU films having different ZnO loadings show similar absorption bands at 2928 cm^{-1}, 1732 cm^{-1}, 1528 cm^{-1}, and 1250 cm^{-1}, which are attributed to the CH_2 anti-symmetric stretching, C=O stretching in urethane and ester, N-H bending plus C-N stretching, and C-O-C stretching in ester, respectively [3, 4]. The variation in the peak intensity is due to thickness differences. The characteristic absorption of ZnO around 500 cm^{-1} was not observed in Figure 2 due to the cut-off of the CaF_2 substrate below 750 cm^{-1}.

The effect of loadings and sizes of ZnO manoparticles on Tg of the ZnO/PU films are displayed in Table 1. A progressive increase in T_g with an increase in particle loading or a decrease in particle size was observed. Given that all systems had similar degrees of dispersion, both increase in loading or decrease in size of the nanoparticles would lead to an increase in the interfacial volume fraction for nanoparticles in the polymer matrix. The increase in T_g of the nanocomposite films suggests a reduction in the mobility of the PU polymer chains [5]. Because T_g can be used to assess the interfacial interactions between nanoparticles and polymers [6], the dependence of T_g on the loading and the size of the nanoparticles indicates that the interactions between ZnO particles and polymers matrix increased with an increase in the interfacial volume fractions in the nanocomposites.

ZnO Loading	Tg (°C)	ZnO Size	Tg (°C)
0%	93.5	None	93.5
1%	114.3	20 nm	127.4
2%	122.6	40 nm	119.8
5%	127.4	60 nm	110.8

Table 1 Effects of loadings and sizes of ZnO nanoparticles on T_g of the ZnO/PU nanocomposite films. For the system with different loadings, the size of ZnO nanoparticle is 20 nm; while for the system with different sizes, the loading of the nanoparticles is 5 %. The T_g value averaged from three specimens. The uncertainties for the data points are less than 2 %.

3.2 Role of Nanoparticles in Long-term Performance of ZnO/ PU Nanocomposites during UV Exposure

Figures 2 and 3 illustrate the effects of loading and size of ZnO nanoparticles on chemical degradation of PU films exposed on SPHERE at 45 °C, 0 % RH. The chemical degradation of the PU is typically represented by the intensity decreases of the bands at 2928 cm^{-1}, 1732 cm^{-1}, 1528 cm^{-1}, and 1041 cm^{-1}. Little change was observed for pure PU films. However, substantial changes were shown for the ZnO/PU films as a function of exposure time. The magnitude of these changes increased with an increase in loading and a decrease in size of the nanoparticles. Note that the specimens exposed to the same temperature/RH condition without UV light showed little degradation. These results indicated that the ZnO nanoparticles used in this study had a photo-catalytic effect on the degradation of PU during SPHERE exposure. This photo-catalytic effect is proposed to be an interface-related phenomenon which increases in magnitude with an increase in the nanoparticle interfacial areas. This hypothesis is further confirmed by EPR results (Figure 4), which shows the photoreactivity of ZnO nanoparticles increased with decreasing nanoparticle size.

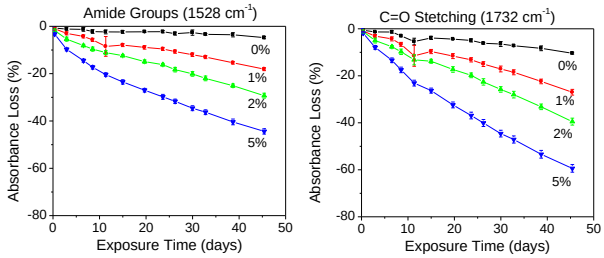

Figure 2: Effect of ZnO nanoparticle loading on chemical degradation of 20 nm ZnO/PU films during exposure on SPHERE at 45 °C, 75 % RH. (A) and (B) represent the absorbance loss of amide II band at 1528 cm^{-1} and C=O stretching band of ester groups at 1732 cm^{-1}, respectively. Each data point in this figure is the average of four specimens, and error bars represent one standard deviation.

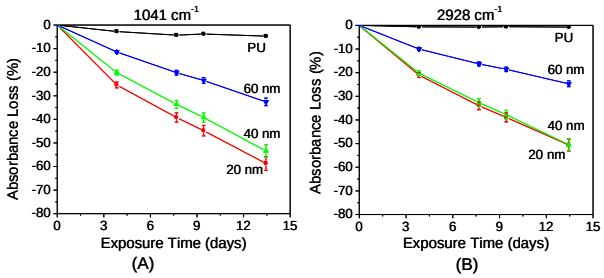

Figure 3: Effect of the nanoparticle size on chemical degradation of 5 % ZnO/PU films exposed on SPHERE at 45 °C, 75 % RH. Three sizes of ZnO particles, 20 nm, 40 nm and 60 nm, were used. (A) and (B) represent absorbance loss of C-O-C asymmetric stretching at 1041 cm^{-1} and CH_2 asymmetric stretching at 2928 cm^{-1}, respectively. Each data point was the average of four specimens, and error bars represent one standard deviation.

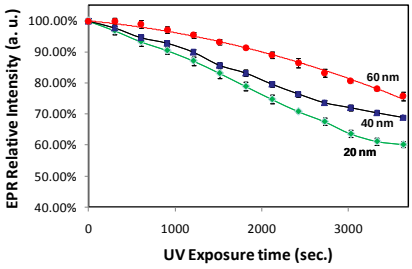

Figure 4: EPR absorbance decay plots using the EPR spin trap method for ZnO nanoparticle dispersions with different particle sizes. Error bars represent one standard deviation.

However, when UVO chamber was used as a UV exposure device, we found that the degradation rate of pure PU was the highest among the films. As shown in Figure 5, when the particle size was fixed at 20 nm, films with 5 %

loading still degraded at a faster rate than the 1 % filled system, but slower than the pure PU films. Further, all three nanoparticle sizes (20 nm, 40 nm and 60 nm) decelerated the degradation of PU films exposed to the UVO condition; that is, they acted as a UV stabilizer. Such a different phenomenon may be attributed to a different degradation mechanism for the specimens exposed to the different UV devices. The short wavelength (i.e., 254 nm and 185 nm) and the consequent atomic oxygen and ozone have caused a different degradation mechanism for specimens exposed to the UVO chamber than those on the SPHERE. In this environment, the role of ZnO nanoparticles has changed: from a photo-catalyst to a photo-stabilizer.

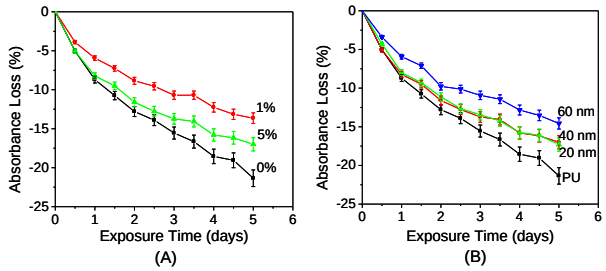

Figure 5: Effect of nanoparticle loading (A) and size (B) on absorbance loss of amide II band at 1528 cm^{-1} as a function of exposure time for ZnO/PU films exposed to UVO cleaner at ambient condition. For the system with different loadings, the size of ZnO nanoparticle is 20 nm; while for the system with different sizes, the loading of the nanoparticles is 5 %. Each data point was the average of four specimens, and error bars represent one standard deviation.

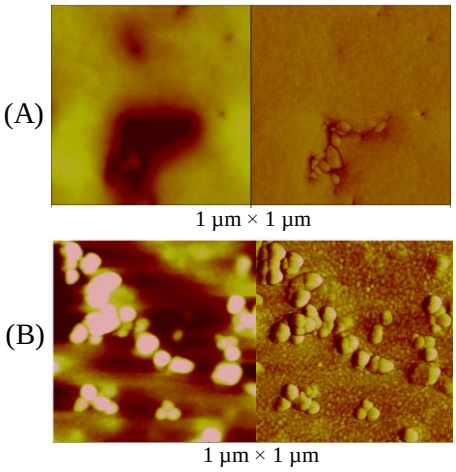

Figure 6: AFM height (left) and phase (right) images for ZnO/PU films exposed to (A) SPHERE at 45 °C, 0 % RH for two months, and (B) UVO chamber in ambient condition for 120 h. Lateral dimensions are 1 μm × 1 μm.

The different roles played by the ZnO nanoparticles in the chemical degradation for ZnO/PU films also resulted in distinctive morphological changes when specimens were exposed to different UV conditions. As shown in Figure 6, for SPHERE exposure, the polymers in the regions surrounding the nanoparticles degraded faster than the bulk polymer matrix, leading to pit formation on the surface of the exposed film (Figure 6A). On the other hand, for UVO chamber exposure, the polymer regions next to the particles changed more slowly than the matrix, forming elevated domains on the film surface. It appeared that the degradation of polymer in the vicinity of the particles was preferentially accelerated when nanoparticles behave as a photo-catalyst, or was protected when nanoparticles act as a photo-stabilizer. Such differences in the local interfacial regions ultimately will result in the overall performance of nanocomposites during exposure to UV irradiation. The results of this study suggested that the nanoparticles play a critical role in the long-term performance and life cycle of nanocomposites.

4 CONCLUSIONS

The role of nanoparticles in a waterborne ZnO/PU system exposed to UV irradiation has been investigated. The effects of loading and size of ZnO nanoparticles on photodegradation of ZnO/PU films were evaluated. The results have shown that ZnO nanoparticles can act as a photo-stabilizer or a photo-catalyst in nanocomposites, depending on the exposure conditions. This study demonstrated that the role of nanoparticles in the life cycle of nanocomposites is critical but also complicated, suggesting that it is necessary to develop new methodologies to accurately predict the service life of these advanced polymer composites.

* Instruments and materials are identified in this paper to describe the experiments. In no case does such identification imply recommendation or endorsement by the National Institute of Standards and Technology (NIST).

REFERENCES

1. C. Hegedus, F. Pepe, D. Lindenmuth, and D Burgard, JCT Coatings Tech, April, 42, 2008.
2. Y.Q. Li, S.Y. Fu, Y.W. Mai, Polymer, 47, 2127, 2006.
3. T. Nguyen, et al. "Service Life Prediction: Challenge the Status Quo," Federation of Societies for Coatings Technology, Blue Bell, PA, 13, 2005.
4. J. Lemaire and N. Siampiringue, "Service Life Prediction of Organic Coatings: A Systems Approach," ACS Symposium Series 772, American Chemical Society, Oxford Press, NY, 198, 1999.
5. D.Y. Perera, Progress in Organic Coatings, 50, 247, 2004.
6. L.S. Schadler, et al. MRS Bulletin, 32, 335, 2007.